

ELECTRONIC SUPPLEMENTARY INFORMATION

Mechanism for the stabilization and surfactant properties of epitaxial silicene

A. Curcella,[†] R. Bernard,[†] Y. Borensztein,[†] M. Lazzeri,[‡] G. Prévot,^{†}*

[†] Sorbonne Universités, UPMC Univ Paris 06, CNRS-UMR 7588, Institut des NanoSciences de Paris, F-75005, Paris, France

[‡] Sorbonne Universités, UPMC Univ Paris 06, CNRS-UMR 7590, MNHN, IRD UMR 206, Institut de Minéralogie, de Physique des Matériaux et de Cosmochimie, F-75005, Paris.

Structural models

In this section we describe the main characteristics of the structural models simulated with density functional theory. The computational details can be found in the main text, which also provides a brief description of the structures and of the given labeling. Figure S1 reports a schematic of the various computed structures. Other configurations were tested. We report only the most stable and/or relevant for the discussion.

Figure S2 reports some of the structural parameters for silver free systems. The meaning of the parameters is described in the inset which represents the BL+Si structure. The BL+Si (ML+Si) structure is a silicene bilayer (monolayer) in which Si atoms have been added on the top to form the $(\sqrt{3} \times \sqrt{3})$ reconstruction. z^{out} is the distance of the added atoms from the outermost Si plane, while z^{ds} is the distance between the added atom and the Si which is immediately below. Note that analogous quantities to z_0 , z_1 and z_2 can be defined for bulk diamond-like Si ("Si bulk"). Concerning the BL-AA structure (not in the Table) we do not obtain major differences with the structural parameters already reported by Pflugradt et al. [1].

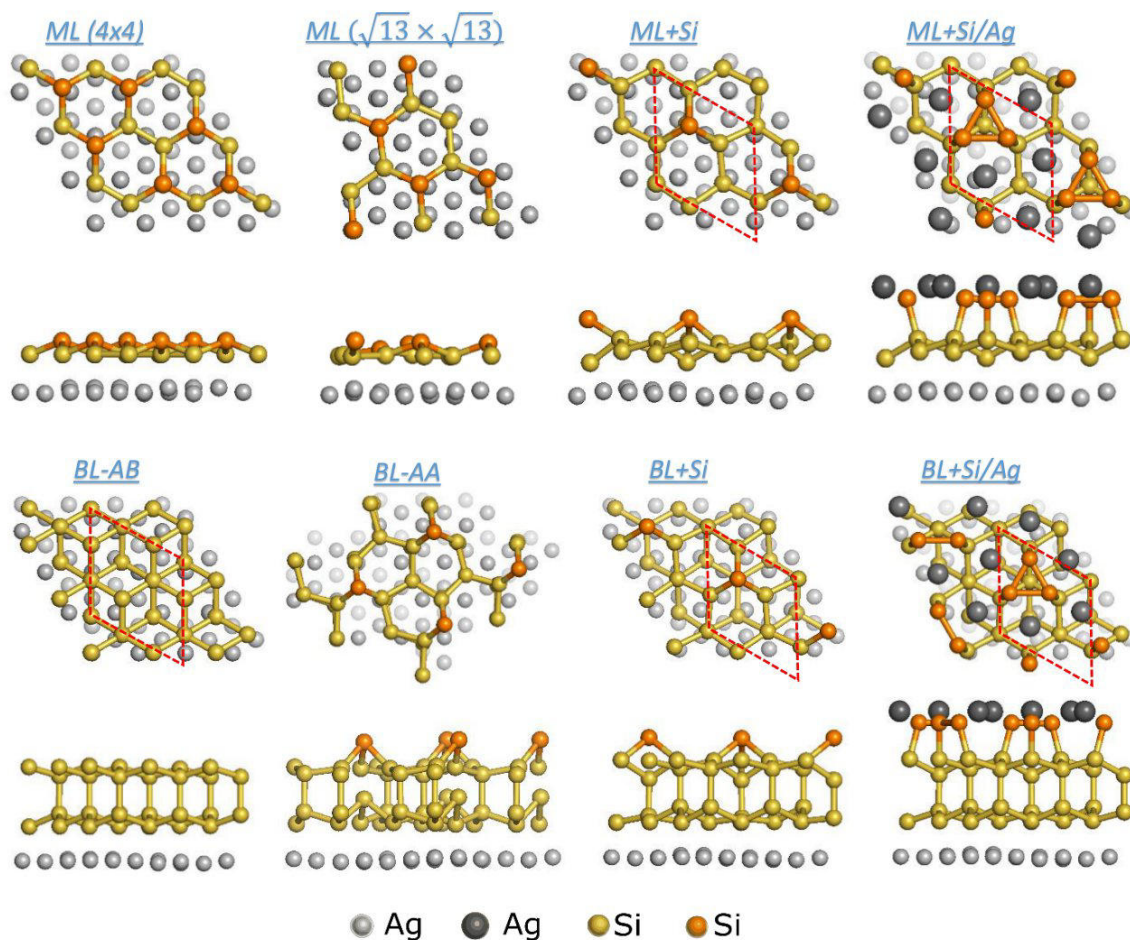


Figure S1: Schematic of the various structures computed. The unit cell is drawn in red for the $(\sqrt{3} \times \sqrt{3})$ reconstructions. For the other structures, it corresponds to the size of the cell.

	Si bulk	ML (4x4)	ML+Si	BL+Si	BL+AB
z^{out}			0.133	0.143	
z^{ds}			0.254	0.265	
z_0	0.079	0.079	0.062	0.053	0.062
z_1	0.237			0.244	0.245
z'_1				0.239	
z_2	0.079			0.096	0.077
z_{Ag}		0.218	0.183	0.228	

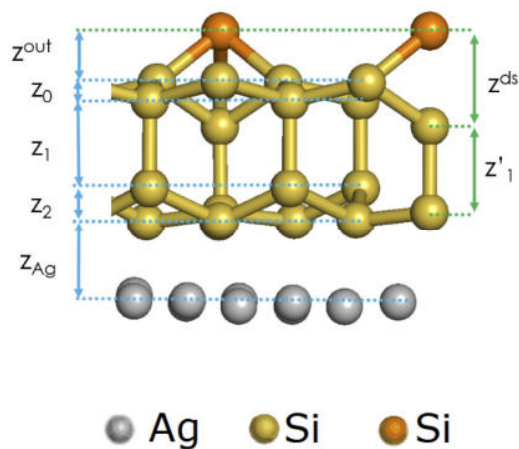


Figure S2: Structural parameters of silver free Si structures. All the values are in nm.

	HCT			IET		
	Si+Ag	ML+Si/Ag	BL+Si/Ag	Si+Ag	ML+Si/Ag	BL+Si/Ag
d_A	0.077	0.072	0.073	0.076	0.080	0.071
d_z	0.230	0.232	0.230	0.230	0.222	0.230
d_0	0.069	0.068	0.065	0.069	0.068	0.065
d'_0	0.100	0.104	0.101	0.100	0.110	0.101
d_1	0.240		0.241	0.240		0.241
d'_1	0.230		0.233	0.230		0.233
d_2	0.086		0.088	0.086		0.088
d_{Ag}		0.239	0.227		0.238	0.233
L_{tr}	0.252	0.252	0.254	0.253	0.254	0.255
L_1	0.351	0.346	0.351	0.302	0.301	0.302
L_2	0.342	0.343	0.351	0.390	0.398	0.398
θ_1				3.8°	3.9°	4.0°
θ_2				5.4°	5.6°	5.5°

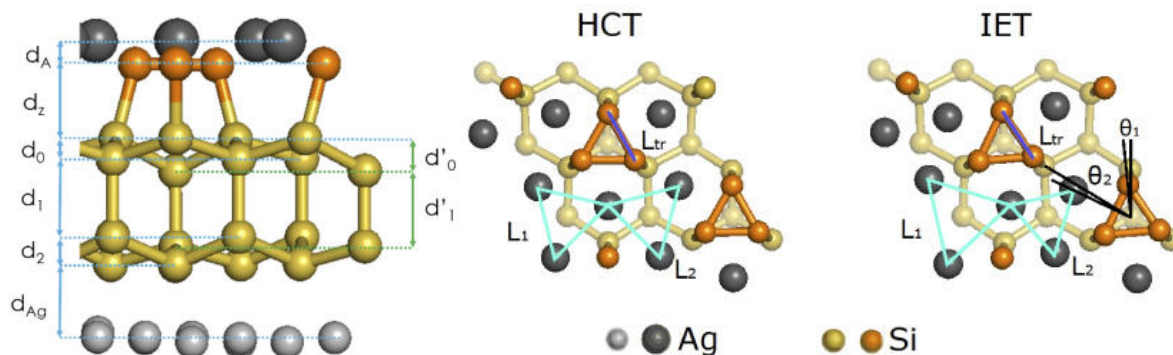


Figure S3: Structural parameters of Ag terminated structures. Distances are expressed in nm.

Figure S3 reports some of the structural parameters for the structures obtained by covering silicene with both Si and Ag atoms in analogy to the $(\sqrt{3} \times \sqrt{3})$ reconstruction observed by covering the Si(111) surface with Ag atoms [2,3]. The meaning of the parameters is described in the inset which represents the BL+Si/Ag structure. The table in Figure S3 also reports the analogous parameter-values for the Ag/Si(111) reconstruction (“Si+Ag”). These structures, which possess or not a mirror plane symmetry, are labeled following the Si diamond literature as HCT (honeycomb chain triangle, symmetric) or IET (inequivalent triangle, non-symmetric). In the table, the quantities labeled as d_i are distances between atomic planes, while L are the lengths

of the edges of the various equilateral triangles schematized in the figure. θ_1 and θ_2 are angles associated with the tilting of the Si trimers and Ag triangles, respectively, in the non-symmetric structures.

STM images of the $(\sqrt{3} \times \sqrt{3})$ Si/Ag reconstructions.

In Figure S4, we compare the simulated STM images of the Si/Ag reconstructions at two different voltages (U). Computational details are the same as in the main text. "Si+Ag" refers to the $(\sqrt{3} \times \sqrt{3})$ reconstruction obtained by covering the Si(111) surface with Ag atoms. For the ML+Si/Ag and BL+Si/Ag structures, we consider only the symmetric configurations (HCT). One should remark that for $U=0.5$ V, the STM images of the HCT and IET Si+Ag structures are very similar to those reported in literature [2]. On the other hand, the shape of this image qualitatively changes by changing U (compare $U=0.5$ V with $U=1.6$ V for the Si+Ag structures in Figure S4). On the contrary, the images of the ML+Si/Ag and BL+Si/Ag do not substantially change upon a variation of U and are quite different from those obtained for Ag/Si(111) ("Si+Ag") at $U=0.5$ V. Concluding, in spite of the fact that the atomic structures of the BL+Si/Ag structure and those of the $(\sqrt{3} \times \sqrt{3})$ reconstruction of Ag/Si(111) ("Si+Ag") are very similar (see Table S3), the calculated STM images at $U=0.5$ V are quite different.

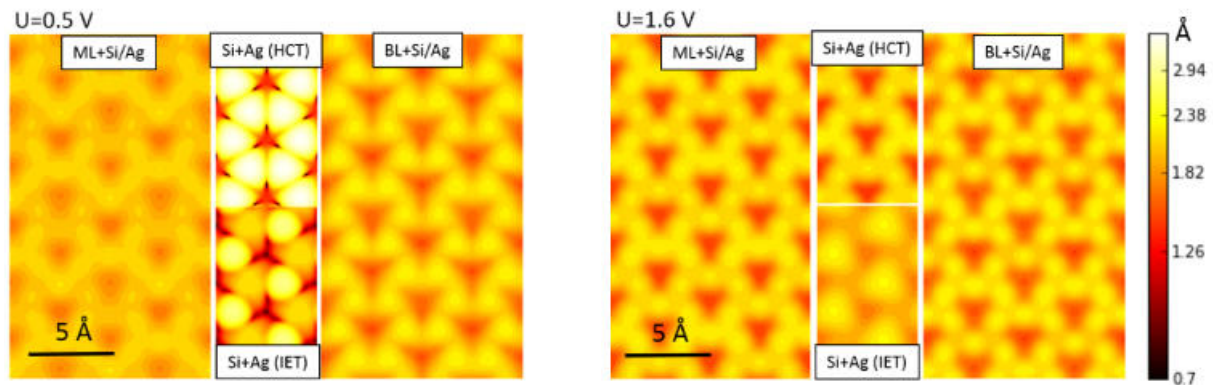


Figure S4: Simulated STM images of various Si/Ag reconstructions for $U=0.5$ V (left panel) and $U=1.6$ V (right panel).

For the Ag-Si(111) case at $U=0.5$ V, we reproduce the images reported in the literature [2], in which the electronic density of states is localized in-between the Ag triangles at the surface. Instead, concerning the BL+Si/Ag structures, both at $U=0.5$ V and $U=1.6$ V, the electronic density of state is localized around the Ag atoms and not in-between the triangles they form.

Energetic of the adsorption of one atom.

Here we report the adsorption energy of one atom over silicene through DFT (computational details are in the main text).

Calculations.

We consider the (4×4) reconstruction of silicene over the Ag(111) surface, simulating the surface with a 4 layers slab ($16 \times 4 + 18 = 82$ atoms per unit cell). The structure has energy $E_{(4 \times 4)}$. We then add one Si atom to the silicene structure. After full atomic position relaxation, the slab has energy E_{+Si} . Various adsorption sites were tested and we report only the most stable here: a Si atom can be added on the top of a Si atom of silicene (sites which in Figure S5 are labeled “t”, note that various inequivalent “t” sites are possible) or on the top of one center of the silicene hexagons (“h” sites in Figure S5). We then consider a Si atom inserted below silicene, substituting one Ag atom (“A” sites in Figure S5), the corresponding energy is E_{+Si-Ag} . As a comparison, we also add one Ag atom on the top of the “h” sites, corresponding to a slab with energy E_{+Ag} . Also in this case various adsorption sites above and below the silicene layer were tested. The “h” sites are most stable. The substitution of a Ag atom with one Si of the silicene crystal is energetically unfavoured and is not discussed. The table in Figure S5 (the upper part) reports the atomic adsorption energies (on various adsorption sites) defined as:

$$\varepsilon_{+Si} = E_{+Si} - E_{(4 \times 4)} - E_{Si}^{blk}$$

$$\varepsilon_{+Si-Ag} = E_{+Si-Ag} - E_{(4 \times 4)} - E_{Si}^{blk} + E_{Ag}^{blk}$$

$$\varepsilon_{+Ag} = E_{+Ag} - E_{(4 \times 4)} - E_{Ag}^{blk}$$

Here, E_{Si}^{blk} is the energy of one Si atom in the diamond bulk and E_{Ag}^{blk} is the energy of one Ag atom in the *fcc* bulk. To make a comparison, the table reports, in the row labeled “Ag(111)”, the three analogous energies obtained after adsorption on the clean Ag surface (these quantities are those already calculated in Ref. [4]) and, in the last row (“Ag_{blk}”), the energy of a substitutional Si atom in a Ag bulk supercell (48 atoms)

Note that in Figure S5 we assume the equivalence of the two C_3 symmetric centers (both labeled “h₁”). In the actual 4×4 reconstruction the two centers are not exactly equivalent because of the presence of deeper layers (not shown in the figure) below the Ag surface plane, and the number of strictly inequivalent sites is roughly double with respect to those reported on the table. For the present purpose, this asymmetry is however slight: the adsorption energies of two slightly inequivalent sites differ by no more than 0.01 eV.

Finally, we also calculated the energy ε_{-Ag} to subtract one of the outermost Ag atoms (on the top of silicene) from the two considered Ag-rich reconstructions labeled as “ML+Si/Ag” and “BL+Si/Ag” in Fig. S1. Let us call $E^{BL+Si/Ag}$ the energy of the slab simulating the BL+Si/Ag reconstruction ($4 \times 16 + 9$ Ag atoms + $2 \times 18 + 9$ Si atoms) and

$E_{-Ag}^{BL+Si/Ag}$ the energy (determined after atomic relaxation) of the same slab in which one of the outermost Ag atoms has been subtracted. Analogous quantities can be defined for the ML+Si/Ag structure. We have:

$$\varepsilon_{-Ag}^{BL+Si/Ag} = E_{-Ag}^{BL+Si/Ag} - E^{BL+Si/Ag} + E_{Ag}^{blk} = +0.49\text{eV}$$

$$\varepsilon_{-Ag}^{ML+Si/Ag} = E_{-Ag}^{ML+Si/Ag} - E^{ML+Si/Ag} + E_{Ag}^{blk} = +0.24\text{eV}$$

These values can be compared with the energy (present calculations) to create a vacancy on the clean Ag(111) surface, $\varepsilon_{-Ag}^{Ag(111)} = +0.59$ eV, and to create a vacancy in the Ag bulk $\varepsilon_{-Ag}^{blk} = +0.78$ eV. The energy to create a Ag vacancy immediately below the silicene 4x4 reconstruction, ε_{-Ag}^{ML} , is defined in analogous way and depends on the Ag site considered. Using the labels of Fig. S5, we obtained $\varepsilon_{-Ag}^{ML} = +0.51, +0.52, +0.084, +0.71$ eV, for the sites A_1, A_2, A_3, A_4 , respectively.

ε_{+Si} (eV)	ε_{+Si-Ag}	ε_{+Ag}
6t ₁ : 0.65	3A ₁ : 0.49	
6t ₂ 1.02	6A ₂ 0.68	
6t ₃ 1.21	1A ₃ 0.79	
2h ₁ 0.62	6A ₄ 0.87	2h ₁ : 0.40
6h ₂ 1.22		6h ₂ 0.64
1h ₃ 1.52		1h ₃ 0.51
Ag(111): 1.27	0.50	0.67
Ag _{blk} : 0.67		

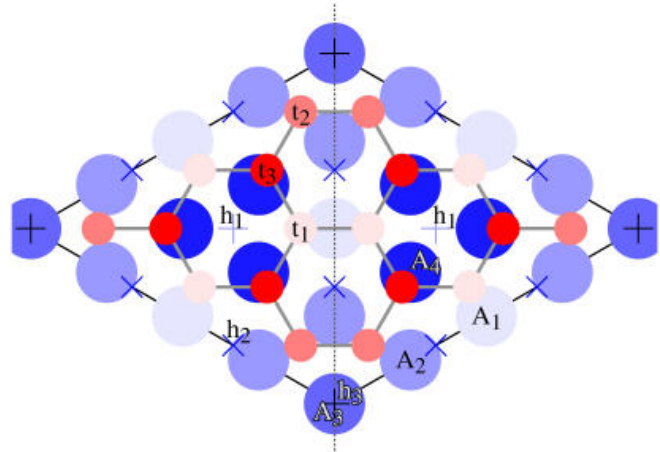


Figure S5: Adsorption energies (eV) on various sites of the 4x4 reconstruction. Labels are defined in the text. The adsorption sites are schematized in the right panel (top view of the system). Bluish circles are Ag atoms of the outermost layer, while reddish ones are Si atoms. The black line represents the 4x4 unit cell. The system has C_3 symmetry around the two sites labeled h_1 . To simplify the notation we assume the presence of mirror symmetry for the plane vertical to the surface and passing through the dotted line (see the text). There are four inequivalent Ag sites labeled A_1, A_2, A_3, A_4 . In the table, the same labels appear preceded by an integer number indicating the number of equivalent sites (e.g. $3A_1$ means that there are three equivalent A_1 sites), which could be identified through the color code of the figure. Using the same notation, there are three inequivalent Si sites: t_1, t_2, t_3 . The crosses indicate the centers of the Si hexagons and are labeled as h_1, h_2, h_3 .

Discussion.

$\epsilon_{+\text{Si}}$ quantifies how much a Si atom prefers to bind on a certain site on the top of the silicene/Ag(111) system. All $\epsilon_{+\text{Si}}$ are >0 , meaning that Si atoms are more stable in the Si bulk. $\epsilon_{+\text{Si-Ag}}$ quantifies how much a Si atom prefers to bind in a certain site (below silicene) after having displaced an Ag atom (which migrates somewhere else, still remaining within the surface). Smaller values correspond to more stable configurations. The most relevant result from the table in Figure S5 is that, among the various values of $\epsilon_{+\text{Si}}$ and $\epsilon_{+\text{Si-Ag}}$, the smallest one corresponds to $\epsilon_{+\text{Si-Ag}}$ (in the A_1 configuration). This means that it is energetically more favorable for a Si atom to insert below the silicene layer (displacing one Ag atom) rather than to stick on the top of silicene. This result is compatible with the experimental observation, reported in the main text, that the silicene bilayer forms by dislodging the atoms of the outermost Ag layer, which is below the original silicene monolayer.

We now consider the energy to create a Ag vacancy below the silicene layer, $\epsilon_{-\text{Ag}}^{\text{ML}}$. These energies can be used to quantify the strength of the Ag-Ag bonds, which is a relevant quantity to better understand the process of formation of the β phase, since this process is associated with the migration of the underlying Ag atoms. The vacancy formation energy on the clean Ag(111) surface, $\epsilon_{-\text{Ag}}^{\text{Ag}(111)}=0.59$ eV, is slightly smaller than the adsorption energy of an Ag atom over the Ag surface (0.67 eV). In principle, one should expect the presence of silicene to stabilize (increase) the energy of the outermost Ag atoms of the surface, because of additional bonding. Indeed, $\epsilon_{-\text{Ag}}^{\text{ML}}=0.71$ eV for the site A_4 (corresponding to the clean Ag atoms almost below the t_3 Si atoms and, probably, more directly involved in the Si-Ag bonding). Surprisingly, for the sites A_1 and A_2 $\epsilon_{-\text{Ag}}^{\text{ML}}$ (0.51 and 0.52 eV) is not substantially changed with respect to the clean surface value $\epsilon_{-\text{Ag}}^{\text{Ag}(111)}=0.59$ eV. Even more surprisingly, for the A_3 site, ($\epsilon_{-\text{Ag}}^{\text{ML}}=0.084$ eV) is smaller (the A_3 site corresponds to Ag atoms directly below the center of one of the Si hexagons and it is, thus, probably less involved in the Si-Ag bonding). We can thus conclude that the presence of a silicene layer on the top of the Ag(111) does not stabilize the Ag atoms as much as one would have expected, and, actually, diminishes the relative stability of certain Ag atoms, possibly favoring the Ag migration process. Changing perspective, the Ag-Si bond on the Ag-rich silicene reconstruction BL+Si/Ag (which in the main text is attributed to the β phase) is relatively strong being $E_{-\text{Ag}}^{\text{BL+Si/Ag}}=0.49$ eV only 0.1 eV smaller than $\epsilon_{-\text{Ag}}^{\text{Ag}(111)}$. The fact that $E_{-\text{Ag}}^{\text{ML+Si/Ag}}=0.24$ eV is smaller is consistent with the conclusion (of the main text) that the Ag-rich reconstruction stabilizes the silicene bilayer but not the monolayer. Note that these values cannot be directly compared to the thermodynamical plot of Fig. 7 (main text), but provide a complementary information.

A similar mechanism has been already proposed to describe the growth of the silicene monolayer on the Ag(111) surface in Ref. [4]. Indeed, if we compare the adsorption of Si on the bare Ag(111) surface (next to last line of the table), $\epsilon_{+\text{Si-Ag}}$ is favored with respect to $\epsilon_{+\text{Si}}$ to such a degree that $\epsilon_{+\text{Si-Ag}} + \epsilon_{+\text{Ag}} < \epsilon_{+\text{Si}}$, meaning that the insertion of one Si atom (within the Ag surface) can be accompanied by the expulsion of one Ag atom which adsorbs on the top of the surface under an energetically favored process. In the present case, this relation does not hold (compare the smaller values available for each one of the three quantities $\epsilon_{+\text{Si-Ag}}$, $\epsilon_{+\text{Ag}}$, and $\epsilon_{+\text{Si}}$ from Figure S5) and the expelled Ag atom (at least in the first stages of the bilayer growth) tends to remain below the silicene within a process probably requiring a high activation barrier.

Note that the insertion energy of a Si inside the Ag bulk ($\epsilon_{+\text{Si}}$ in the last line of the table) is higher than $\epsilon_{+\text{Si-Ag}}$ for both the Ag(111) surface and for the A_1 site below silicene. This means that, as expected, in both cases, a Si atom that has inserted in the outermost layers of the surface does not have the tendency to migrate below.

Finally, although the process is energetically favored, it is not evident how a Si atom added on the top of the (4×4) silicene/Ag(111) surface can pass through silicene and insert within the Ag surface. The process should be associated with a relevant activation barrier since it implies the displacement of Ag atoms. Possible adsorption dynamics for the free-standing silicene are discussed in Ref. [5]. However, for the present silicene/Ag(111) case, the dynamics is expected to be substantially different. Indeed, if we look at silicene from the top, we can distinguish between inward-buckled (t_1 and t_2 sites in Figure S5) and outward-buckled (t_3) Si atoms. The adsorption of one Si atom on the top of the inward-buckled atoms is favored. This is true for (4×4) silicene/Ag(111), Figure S5, and also for free-standing silicene [5]. However, the relative position of the inward-buckled (IB) and outward-buckled (OB) sites is different: in free-standing silicene, each IB is surrounded by three OB sites; on the contrary, in (4×4) silicene/Ag(111) each IB site has at least one other IB site among the three neighbors (e.g. the two t_1 sites in the middle of Figure S5 are adjacent). Once a Si atom has adsorbed on an IB site of (4×4) silicene/Ag(111) it is, possibly, allowed to jump to neighboring sites with similar adsorption energy. Moreover, in the case of (4×4) silicene/Ag(111), the adsorption on h_1 sites is particularly favored. This kind of adsorption sites is not expected to be relevant in the case of free-standing silicene (the small energy for the h_1 sites in Figure S5 is a direct consequence of the presence of the Ag surface). The h_1 sites are adjacent to the t_1 sites and we can also argue that, because of the very similar energy, the adsorbed atom is allowed to jump from the h_1 to the t_1 site and vice versa.

Concluding, we can imagine that once a Si atom has stucked on the top of the surface on an energetically favored site (t_1 , h_1 or t_2), it is allowed to diffuse by jumps from one site to the other still remaining on the top of the surface. Because of the presence of these diffusion channels on silicene/Ag(111) the adsorbed Si atom could finally reach

a particularly favored location (possibly a step or a defect) to insert below the silicene layer.

REFERENCES

1. Pflugradt, P., Matthes, L. & Bechstedt, F. Unexpected symmetry and AA stacking of bilayer silicene on Ag(111). *Phys. Rev. B* **89**, 205428 (2014).
2. Aizawa, H., Tsukada, M., Sato, N. & Hasegawa, S. Asymmetric structure of the Si (111)- $\sqrt{3}\times\sqrt{3}$ -Ag surface. *Surf. Sci.* **429**, L509-L514 (1999).
3. Takahashi, T. & Nakatani, S. Refinement of the Si (111) $\sqrt{3}\times\sqrt{3}$ -Ag structure by surface X-ray diffraction. *Surf. Sci.* **282**, 17-32 (1993).
4. Bernard, R., Borensztein, Y., Cruguel, H., Lazzeri & Prevot, G. Growth mechanism of silicene on Ag(111) determined by scanning tunneling microscopy measurements and ab initio calculations. *Phys. Rev. B* **92**, 045415 (2015).
5. Cahangirov, S. et al. Atomic structure of the 3×3 phase of silicene on Ag(111). *Phys. Rev. B* **90**, 035448 (2014).